Document to understand the basics of Hyperspectral sensing and aid in it’s selection

Date: 16-1-2019/ Joe Johnson, IIT Mandi

Agricultural Remote Sensing Basics

John Nowatzki , dec 2011

https://articles.extension.org/pages/9693/agricultural-remote-sensing-basics

Remotely sensed images can be used to identify nutrient deficiencies, diseases, water deficiency or surplus, weed infestations, insect damage, hail damage, wind damage, herbicide damage, and plant populations.

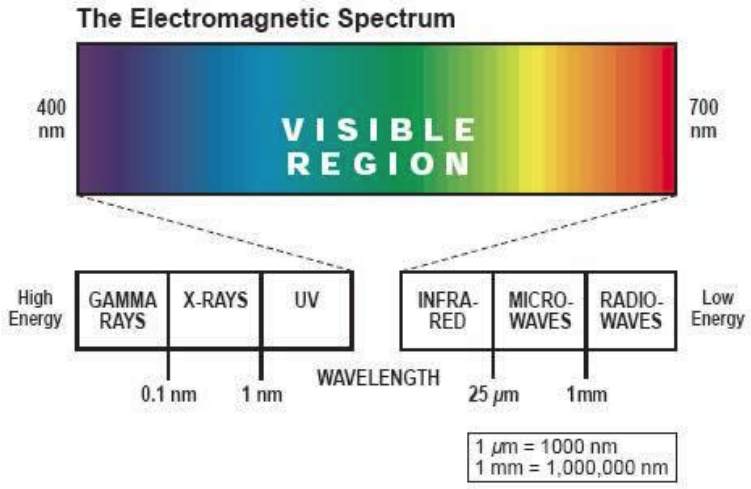

Figure 1. The visible region of the spectrum ranges from about 0.4 μm to 0.7 μm (Kyllo, 2004).

Wavelengths longer than those in the visible region and up to about 25 μm are in the infrared region. The infrared region nearest to that of the visible region is the near infrared (NIR) region. Both the visible and infrared regions are used in agricultural remote sensing.

Interactions between reflected, absorbed, and transmitted energy can be detected by remote sensing.The differences in leaf colors, textures, shapes, or even how the leaves are attached to plants, determine how much energy will be reflected, absorbed or transmitted. The relationship between reflected, absorbed, and transmitted energy is used to determine spectral signatures of individual plants. Spectral signatures are unique to plant species.

Stressed sugar beets have a higher reflectance value in the visible region of the spectrum from 400 to 700 nm. This pattern is reversed for stressed sugar beets in the nonvisible range from about 750 to 1,200 nm. The visible pattern is repeated in the higher reflectance range from about 1,300 to 2,400 nm.

The comparison of the reflectance values at different wavelengths, called a vegetative index, is commonly used to determine plant vigor. The most common vegetative index is the normalized difference vegetative index (NDVI). NDVI compares the reflectance values of the red and NIR regions of the electromagnetic spectrum. The NDVI value of each area on an image helps identify areas of varying levels of plant vigor within fields.

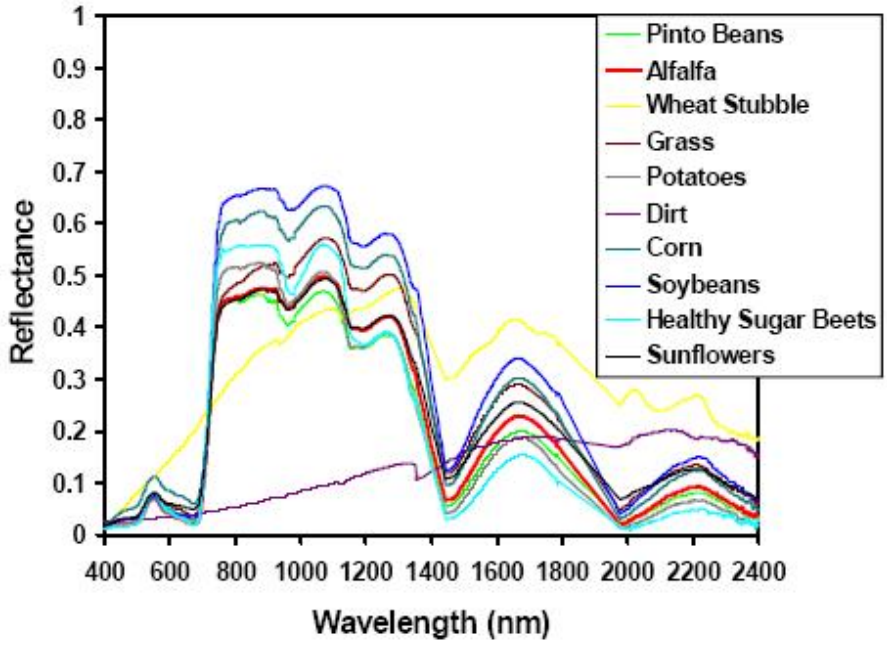

Figure 2. Spectral signatures of crops and soil (Kyllo, 2003).

Spatial resolution refers to the size of the smallest object that can be located in fields or detected in an image. The basic unit in an image is called a pixel.

Spectral resolution refers to the number of bands and the wavelength width of each band. A band is a narrow portion of the electromagnetic spectrum. Shorter wavelength widths can be distinguished in higher spectral resolution images.

Radiometric resolution refers to the sensitivity of a remote sensor to variations in the reflectance levels. The higher the radiometric resolution of a remote sensor, the more sensitive it is to detecting small differences in reflectance values. Higher radiometric resolution allows a remote sensor to provide a more precise picture of a specific portion of the electromagnetic spectrum.

Temporal resolution refers to how often a remote sensing platform can provide coverage of an area. Geostationary satellites can provide continuous sensing while normal orbiting satellites can only provide data each time they pass over an area. Remote sensing taken from cameras mounted on airplanes is often used to provide data for applications requiring more frequent sensing.Remote sensors located in fields or attached to agricultural equipment can provide the most frequent temporal resolution.

Application of hyperspectral imaging and chemometrics for variety classification of maize seeds, Yiying Zhao, Dec 2017

A hyperspectral imaging system covering the spectral range of 874–1734 nm was applied for variety classification of maize seeds.

Spectral data of 975.01– 1645.82 nm were extracted and preprocessed.

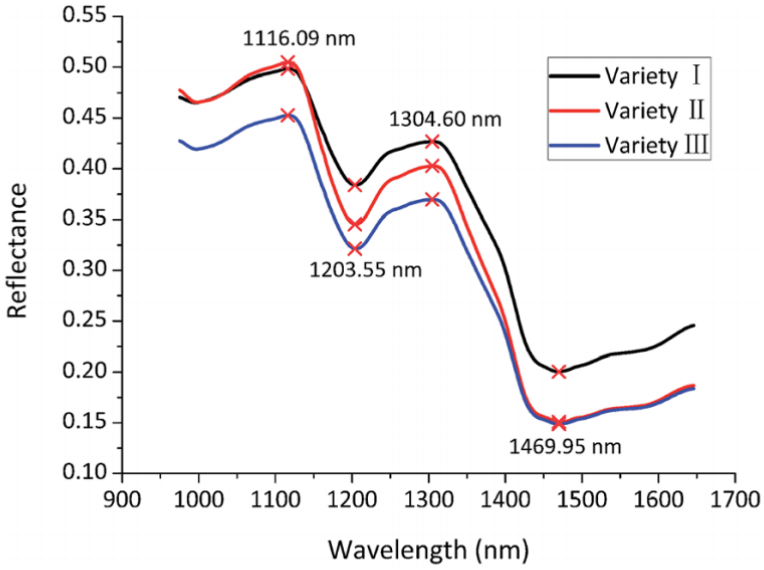

Fig. 1 Average reflectance spectra of maize seeds of three varieties in the range of 975.01–1645.82 nm.

Utility of Hyperspectral Data for Potato Late Blight Disease Detection, Shibendu Shankar Ray,2011

https://www.researchgate.net/publication/226357711_Utility_of_Hyperspectral_Data_for_Potato_Late_Blight_Disease_Detection

The study was carried out to investigate the utility of hyperspectral reflectance data for potato late blight disease detection.
The hyperspectral data was collected for potato crop at different level of disease infestation using hand-held spectroradiometer over the spectral range of 325-1075 nm.
The data was averaged into 10-nm wide wavebands, resulting in 75 narrowbands. The reflectance curve was partitionedinto five regions, viz. 400–500 nm, 520–590 nm, 620–680 nm, 770–860 nm and 920–1050 nm.
The notable differences in healthy and diseased potato plants were noticed in 770–860 nm and 920–1050 nm range.
The optimal hyperspectral wavebands to discriminate the healthy plants from disease infested plants were 540, 610, 620, 700, 710, 730, 780 and 1040 nm whereas upto 25% infestation could be discriminated using reflectance at 710, 720 and 750 nm.

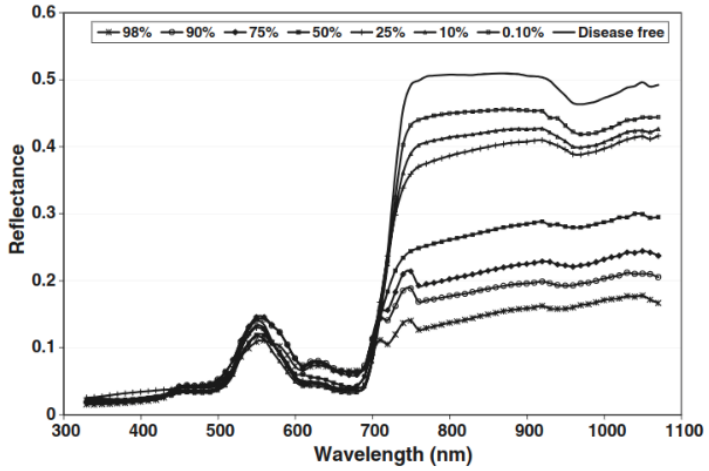

Fig. 1 Reflectance of potato crop at different level of late blight infestation

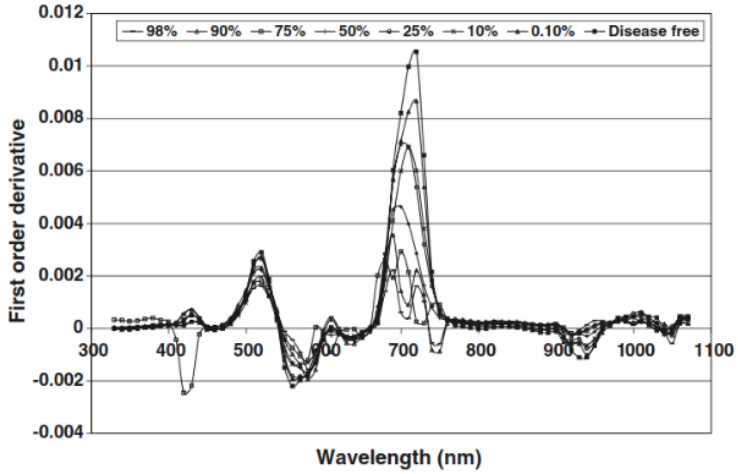

Fig. 2 First order derivative spectra of reflectance of late blight infestation

Table 3 Average spectral reflectance of potato crop under different level of infestation

Ranges (nm)	Disease free	Diseased plants						
		0.10%	10%	25%	50%	75%	90%	98%
400–500	0.0357	0.0316	0.0300	0.0400	0.0312	0.0363	0.0369	0.0343
520–590	0.1058	0.1020	0.0902	0.1019	0.0970	0.1222	0.1205	0.0965
620–680	0.0404	0.0427	0.0378	0.0456	0.0497	0.0680	0.0713	0.0688
770–860	0.5074	0.4505	0.4159	0.3899	0.2649	0.2060	0.1802	0.1406
920–1050	0.4810	0.4332	0.4128	0.4014	0.2877	0.2309	0.2012	0.1673
Absolute Differences from disease free plants								
400–500		0.0041	0.0057	−0.0043	0.0045	−0.0006	−0.0012	0.0014
520–590		0.0038	0.0156	0.0038	0.0088	−0.0164	−0.0147	0.0093
620–680		−0.0022	0.0026	−0.0052	−0.0092	−0.0275	−0.0309	−0.0283
770–860		0.0569	0.0915	0.1175	0.2426	0.3014	0.3272	0.3668
920–1050		0.0478	0.0682	0.0795	0.1933	0.2501	0.2798	0.3137
Percentage differences from disease free plants								
400–500		11.40	15.87	−12.13	12.56	−1.64	−3.38	3.88
520–590		3.57	14.74	3.63	8.33	−15.53	−13.88	8.76
620–680		−5.45	6.47	−12.77	−22.76	−68.05	−76.37	−69.98
770–860		11.21	18.04	23.16	47.80	59.40	64.49	72.29
920–1050		9.93	14.17	16.54	40.19	51.99	58.18	65.22

ıntercomparison of Unmanned Aerial Vehicle and Ground-Based Narrow Band Spectrometers Applied to Crop Trait Monitoring in Organic Potato Production, Marston Héracles Domingues Franceschini, 2017

https://www.ncbi.nlm.nih.gov/pmc/articles/PMC5492811/pdf/sensors-17-01428.pdf

Hyperspectral data was acquired during the growing season using the WageningenUR Hyperspectral Mapping System (HYMSY), an UAV-based pushbroom imaging system [24]. It comprises a custom spectrometer (PhotonFocus SM2-D1312 camera – PhotonFocus AG, Lachen, SZ, Switzerland – with a Specim ImSpector V10 2/3 spectrograph – Specim, Spectral Imaging Ltd., Oulu, Finland), a photogrammetric camera (Panasonic GX1 16 MP – Panasonic Corp., Osaka, Japan – with 14 mm pancake lens), an integrated GPS and inertial navigation system (INS) unit (XSens MTi-G-700 – Xsens Technologies BV, Enschede, The Netherlands), together with synchronization and data sink elements. The equipment weights approximately 2 kg.

Table 2. Vegetation indices used to estimate crop traits.

Vegetation Index	Formulation [1]	Spectral Bands (Centre-nm)		Sensitive to (Scale) [2]	Re
		Ground	UAV		
NDVI	$\frac{R_{800}-R_{670}}{R_{800}+R_{670}}$	670, 780	670, 800	chl, LAI, chl × LAI (L, C)	[68
WDVI	$R_{870} - C\,R_{670}$; $C = \frac{RSoil_{870}}{RSoil_{670}}$	670, 870	670, 870	LAI (C)	[47
OSAVI	$(1+0.16)\frac{(R_{800}-R_{670})}{(R_{800}+R_{670}+0.16)}$	670, 780	670, 800	chl, LAI, chl × LAI (L, C)	[46
MCARI	$[(R_{700}-R_{670})-0.2(R_{700}-R_{550})]\left(\frac{R_{700}}{R_{670}}\right)$	550, 670, 700	550, 670, 700	chl (L)	[20
TCARI	$3\left[(R_{700}-R_{670})-0.2(R_{700}-R_{550})\left(\frac{R_{700}}{R_{670}}\right)\right]$	550, 670, 700	550, 670, 700	chl (L)	[49
MCARI/OSAVI	$\frac{[(R_{700}-R_{670})-0.2(R_{700}-R_{550})]\left(\frac{R_{700}}{R_{670}}\right)}{(1+0.16)\frac{(R_{800}-R_{670})}{(R_{800}+R_{670}+0.16)}}$	550, 670, 700, 780	550, 670, 700, 800	chl (L)	[20
TCARI/OSAVI	$\frac{3\left[(R_{700}-R_{670})-0.2(R_{700}-R_{550})\left(\frac{R_{700}}{R_{670}}\right)\right]}{(1+0.16)\frac{(R_{800}-R_{670})}{(R_{800}+R_{670}+0.16)}}$	550, 670, 700, 780	550, 670, 700, 800	chl (L)	[51
$MCARI_{re}$	$[(R_{750}-R_{705})-0.2(R_{750}-R_{550})]\left(\frac{R_{750}}{R_{705}}\right)$	550, 700, 750	550, 705, 750	chl (L)	[52
$MCARI/OSAVI_{re}$	$\frac{[(R_{750}-R_{705})-0.2(R_{750}-R_{550})]\left(\frac{R_{750}}{R_{705}}\right)}{(1+0.16)\frac{(R_{750}-R_{705})}{(R_{750}+R_{705}+0.16)}}$	550, 700, 750	550, 705, 750	chl (L)	[52
$TCARI/OSAVI_{re}$	$\frac{3\left[(R_{750}-R_{705})-0.2(R_{750}-R_{550})\left(\frac{R_{750}}{R_{705}}\right)\right]}{(1+0.16)\frac{(R_{750}-R_{705})}{(R_{750}+R_{705}+0.16)}}$	550, 700, 750	550, 705, 750	chl (L)	[52
CI_{re}	$\frac{R_{780}}{R_{710}}-1$	710, 780	710, 780	chl (L)	[54,5
CI_g	$\frac{R_{780}}{R_{550}}-1$	710, 750	710, 750	chl (L)	[54,5
MCARI2	$\frac{1.5[2.5(R_{800}-R_{670})-1.3(R_{800}-R_{550})]}{\sqrt{(2R_{800}+1)^2-(6R_{800}-5\sqrt{R_{670}})-0.5}}$	550, 670, 780	550, 670, 800	LAI (C)	[67
REP	$700+40\frac{\left(\frac{R_{670}+R_{780}}{2}\right)-R_{700}}{R_{740}-R_{700}}$	670, 700, 740, 780	670, 700, 740, 780	chl, LAI, chl × LAI (L, C)	[55
MTCI	$\frac{R_{754}-R_{709}}{R_{709}-R_{681}}$	670, 710, 750	680, 710, 755	chl, LAI, chl × LAI (L, C)	[57
PRI	$\frac{R_{570}-R_{531}}{R_{570}+R_{531}}$	530, 570	530, 570	xan, car, car/chl, LAI (L, C)	[60

[1] R_w = reflectance in the spectral band centered in w, $RSoil_w$ = reflectance of bare soil in the spectral band centered in w; [2] chl = leaf chlorophylls content; LAI = leaf area index; chl × LAI = canopy chlorophylls content; xan = xantophylls; car = carotenoids; car/chl = ratio between carotenoids and chlorophylls; L = leaf scale; C = canopy scale.

LAI assessment of wheat and potato crops by VENμS and Sentinel-2 bands, I. Herrmann,2011
http://www.bgu.ac.il/bidr/research/phys/remote/Papers/2011-Herrmann_LAI-VENuS-Sentinel_RSE_11.pdf

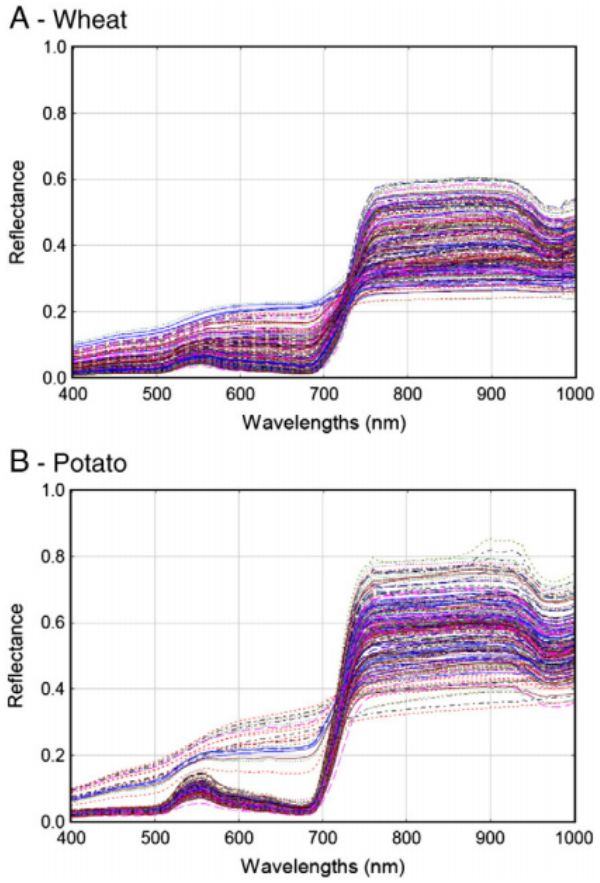

Fig. 2. Spectral variation of reflectance curves: (A) Wheat and (B) Potato.

Detection of Corn and Weed Species by the Combination of Spectral, Shape and Textural Features, Fenfang Lin, 2017

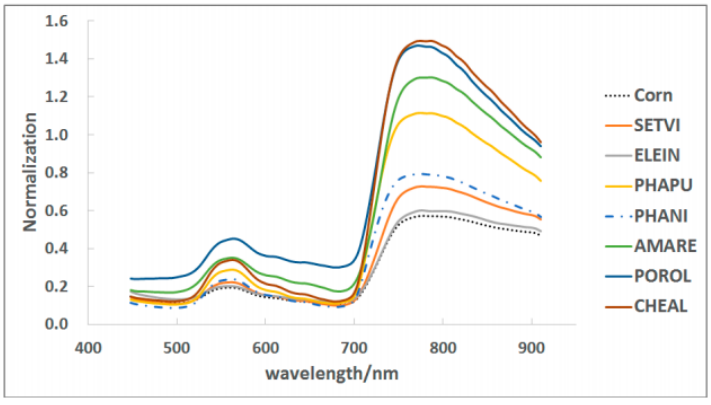

Figure 3. Spectral response curves of corn and seven weed species. Each curve is the mean of normalized values in all leaf images of each plant after data preprocessing. SETVI: foxtail, ELEIN: goosegrass, PHAPU: round leaf pharbitis, PHANI: lobed leaf pharbitis, AMARE: redroot amaranth, POROL: purslane, CHEAL: lambs quarters.

Canopy Vegetation Indices from In situ Hyperspectral Data to Assess Plant Water Status of Winter Wheat under Powdery Mildew Stress, Wei Feng,2017

-FieldSpec HandHeld spectrometer (Analytical Spectral Devices Inc., Boulder, Colorado, USA) over 350–2,500 nm spectral region, at 0.5 m above the wheat canopy with a field of view of 25◦ (Cao et al., 2013), and a spectral sampling interval of 1.4 nm for the 350–1,050 nm region and 2 nm for the 1,000–2,500 nm region. Each spectrum measurement was carried out under sunny and windless conditions at 10:00–14:00 local time. For each sampling point, a view area of ∼0.17 m2 of wheat canopy was selected to measure canopy reflectance spectra, five sequential readings were averaged to obtain one spectrum, and to analyze biochemical and biophysical canopy features.

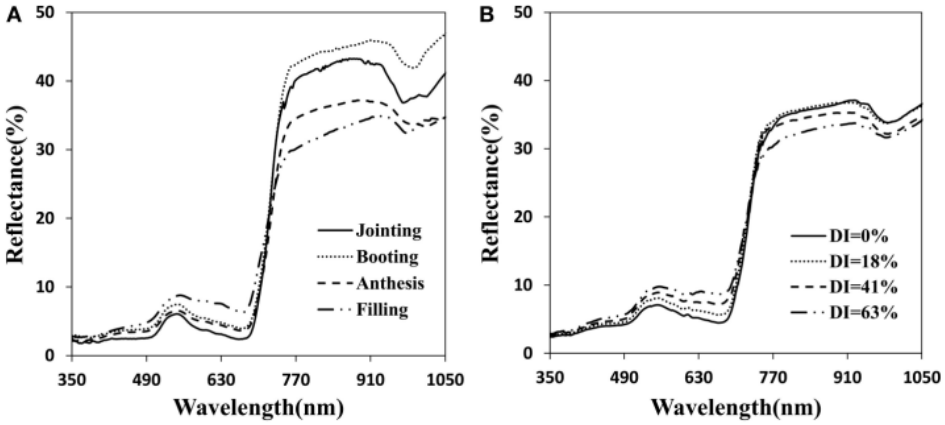

FIGURE 3 | Canopy reflectance spectra for the different infected developmental stages **(A)** and for different disease index of powdery mildew at anthesis **(B)**.

Band Selection of Hyperspectral Images Based on Bhattacharyya Distance, CAI SIMIN, 2009

http://www.wseas.us/e-library/transactions/information/2009/29-322.pdf

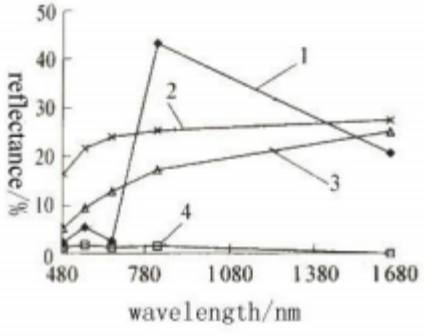

(a) Multispectral curve

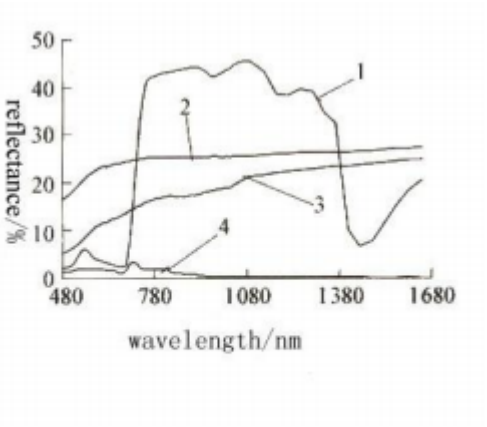

(b) Hyperspectral curve

1 Vegetation 2. Road 3. Bare soil 4. Water body

Selection of Hyperspectral Narrowbands (HNBs) and Composition of Hyperspectral Twoband Vegetation Indices (HVIs) for Biophysical Characterization and Discrimination of Crop Types Using Field Reflectance and Hyperion/EO-1 Data, Prasad S. Thenkabail, 2013
https://ieeexplore.ieee.org/stamp/stamp.jsp?tp=&arnumber=6507245

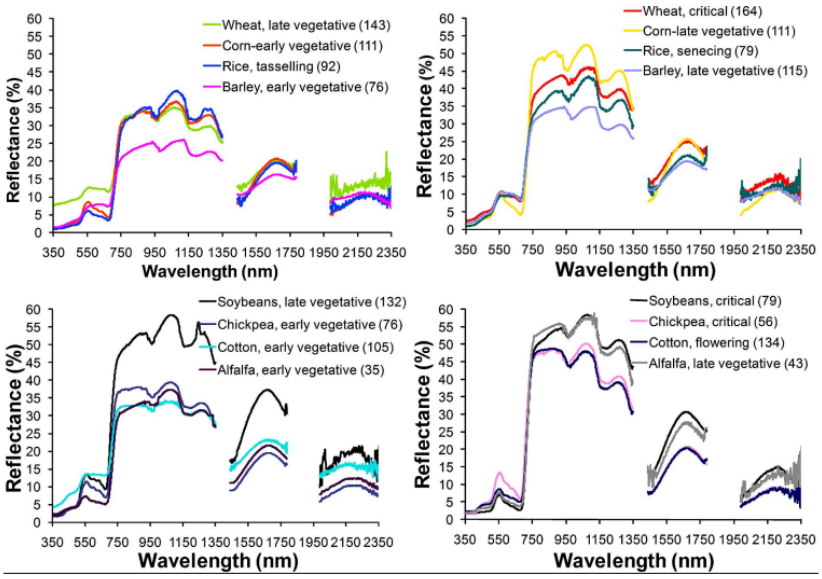

Fig. 2. Cross-site hyperspectral spectroradiometer data. Cross-site mean (regardless of which study site (1–4, Table II)) spectral plots of eight leading world crops in various growth stages. (A) Four crops at different growth stages; (B) same four crops as in A but in different growth stages; (C) four more crops at early growth stages; and (D) same four crops as C, but at different growth stages. Note: numbers in bracket are sample sizes.

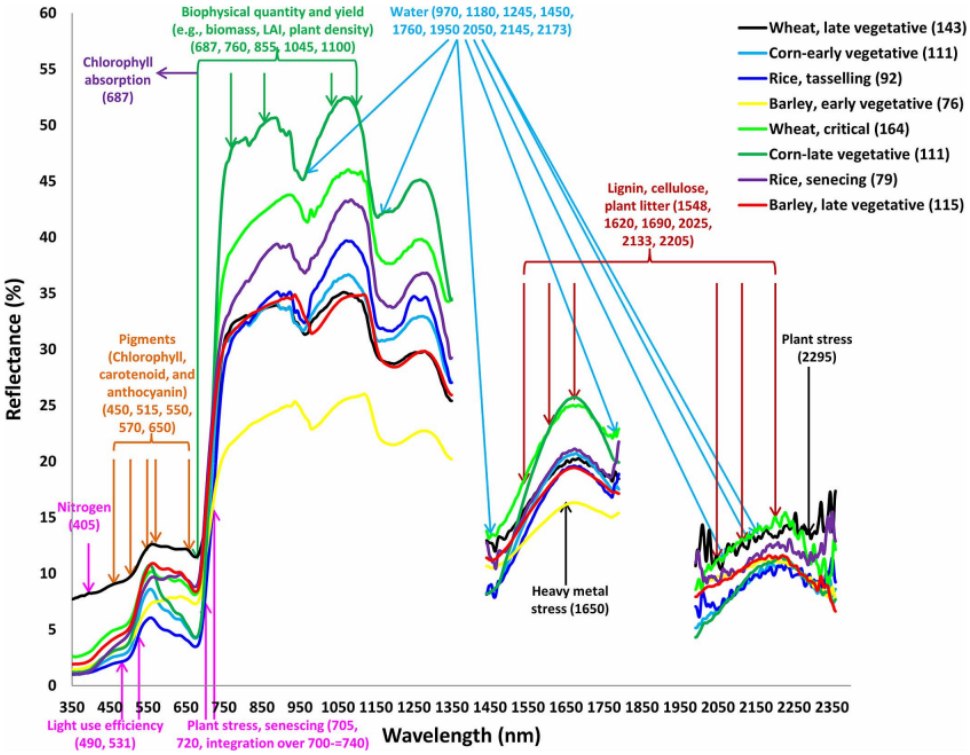

Fig. 8. Optimal hyperspectral narrowbands (HNBs). Current state of knowledge on hyperspectral narrowbands (HNBs) for agricultural and vegetation studies (inferred from [8]). The whole spectral analysis (WSA) using contiguous bands allow for accurate retrieval of plant biophysical and biochemical quantities using methods like continuum removal. In contrast, studies on wide array of biophysical and biochemical variables, species types, crop types have established: (a) optimal HNBs band centers and band widths for vegetation/crop characterization, (b) targeted HVIs for specific modeling, mapping, and classifying vegetation/crop types or species and parameters such as biomass, LAI, plant water, plant stress, nitrogen, lignin, and pigments, and (c) redundant bands, leading to overcoming the Hughes Phenomenon. These studies support hyperspectral data characterization and applications from missions such as Hyperspectral Infrared Imager (HyspIRI) and Advanced Responsive Tactically Effective Military Imaging Spectrometer (ARTEMIS). Note: sample sizes shown within brackets of the figure legend refer to data used in this study.

TABLE IV

OPTIMAL HYPERSPECTRAL NARROWBANDS (HNBS) AND VEGETATION INDICES (HVIS) TO STUDY MAJOR WORLD CROPS BASED ON THE λ VERSUS λ R^2-PLOTS INVOLVING HNBS OR HVIS WITH BIOPHYSICAL PARAMETER BASED ON THIS STUDY AND META-ANALYSIS. (ADOPTED FROM [8])

Sl. number #	Waveband centers λ nm	Waveband widths Δλ nm	Hyperspectral Vegetation Indices (HVIs) normalized HVIs*** dimensionless
A. Blue bands			**1. Biophysical indices ((biomass, LAI, plant density, yield)**
1	405	5	HVI REDND1=(855-687)/(855+687) [27,30,31]
2	450	5	HVI REDND2=(855-650)/(855+650) [25,30,31]
3	490	5	HVI REDND3=(760-687)/(760+687) [25,30,31]
B. Green bands			HVI REDND4=(760-650)/(760+650) [25,30,31]
4	515	5	HVI GREENND1=(550-687)/(550+687) [4,5,13]
5	531	1	HVI GREENND2=(550-650)/(550+650) [3,13,25]
6	550	5	HVI FNIRND1=(1045-687)/(1045+687) [27,29,33]
7	570	5	HVI FNIRND2=(1045-650)/(1045+650) [27,29,33]
C. Red bands			HVI FNIRND3=(1245-687)/(1245+687) [7,10,30]
8	650	5	HVI FNIRND4=(1245-650)/(1245+650) [7,10,27]
9	687	5	HVI SWIRND1=(1650-687)/(1650+687) [7,10,31]
D. Red-edge bands			HVI SWIRND2=(1650-650)/(1650+650) [7,10,31]
10	705	5	HVI SWIRND3=(2205-687)/(2205+687) [14,24,30]
11	720	5	HVI SWIRND4=(2205-650)/(2205+650) [14,30,31]
12	700-740	700-740 (integrate)	**2. Biochemical indices ((carotenoids, anthocyanins, chlorophyll)**
E. Near infrared (NIR) bands			HVI Car1=(550-515)/(550+515) [4,5,10]
13	760	5	HVI Car2=(550-687)/(550+687) [27,30,31]
14	855	20	HVI Antho1=(720-550)/(720+550) [7,11,27]
15	970	10	HVI Antho2=(550-515)/(550+515) [10,23]
16	1045	5	HVI Antho3=(855-550)/(855+550) [4,5,14]
E. Far near infrared (FNIR) bands			HVI Antho4=(550-687)/(550+687) [4,5,14]
17	1100	5	HVI Chl1=(855-720)/(855+720) [27,30,31]
18	1180	5	**3. Plant stress indices**
19	1245	5	HVI REDEDGE1=(760-720) [7,25,30]
F. Early short-wave infrared (ESWIR) bands			HVI REDEDGE2=(760-720)/(760-720) [24,25,31]
20	1450	5	HVI REDEDGE3=first-order integrated spectra over 700 to 740 [25,30,31]
21	1548	5	**4. Plant Water and moisture indices**
22	1620	5	HVI WATER1=(855-970)/(855+970) [24,25,30]
23	1650	5	HVI WATER2=(1100-970)/(1100+970) [3,7,27]
24	1690	5	HVI WATER3=(1100-1180)/(1100+1180) [3,27,30]
25	1760	5	HVI WATER4=(1245-1180)/(1245+1100) [24,25,29]
G. Far short-wave infrared (FSWIR) bands			HVI WATER5=(1650-1450)/(1650+1450) [14,23,27]
26	1950	5	HVI WATER6=(2205-1450)/(2205+1450) [14,25,30]
27	2025	5	HVI WATER7=(2205-1950)/(2205+1950) [3,24,29]
28	2050	5	**5. Light use efficiency (LUE)**
29	2133	5	HVI LUE1=(570-531)/(570+531) [6,27,30]
30	2145	5	**6. Legnin, Cellulose, Residue index**
31	2173	5	HVI LCR1=(2205-2025)/(2205+2025) [14,27,30]
32	2205	5	
33	2295	5	

*** = For broader physical/biological understanding of these indices refer to the references cited next to each index or to various chapters in the book [8].

https://surfaceoptics.com/applications/precision-agriculture-hyperspectral-sensors/

Some of the benefits of hyperspectral and multispectral imaging are that these technologies are: low cost (when compared with traditional scouting methods), give consistent results, simple to use, allow for rapid assessments, non-destructive, highly accurate, and have a broad range of applications.

The ability of hyperspectral imaging to provide valuable data on the condition and health of crops is predicated on the interaction and relationship between electromagnetic radiation (EMR) and foliage.

In the red and blue parts of the visible spectrum, reflectance is primarily a result of absorption by the photosynthetic pigments.

Water content is the primary influence on reflectance in the mid-infrared (MIR) while reflectance in the near-infrared area (NIR) is influenced by the shape and condition of air spaces in the spongy mesophyll.

Senescence, nutrient stress, pathogen and insect infestation have all been shown to significantly reduce reflectance in the mid-infrared spectral region.

It has been well recorded that a vegetation index of NIR and red wavelengths can monitor a range of plant-health issues including fungal pathogens, excess salt and nutrient deficiencies.

One of the most powerful techniques for the measurement of overall photosynthetic efficiency and thus of plant productivity, is the fluorescence of chlorophyll a in photosystem II.

zeaxanthin pigment is produced by plants to safely remove excess photons when light intensity exceeds the ability of photosystem II to absorb photons without becoming over-energized. Zeaxanthin accumulation can therefore be used as a quantitative indicator of non-photochemical energy dissipation and therefore of light-use efficiency.

By measuring changes at waveband 531nm, which is affected by the production of zeaxanthin and comparing it with waveband 570 nm, which is not affected, a standard Photochemical Reflectance Index (PRI) has been developed which serves as a measure of photosynthetic light use efficiency.

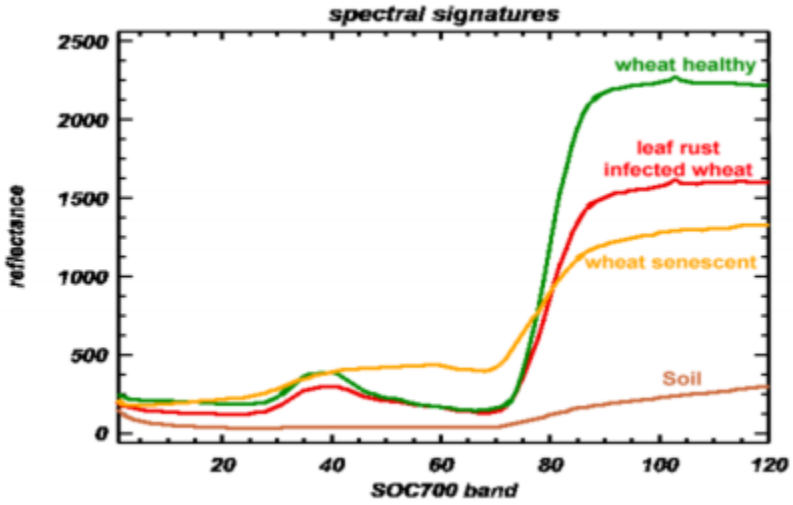

multispectral imagery generally ranges from 5 to 12 bands that are represented in pixels and each band is acquired using a remote sensing radiometer, hyperspectral imagery consists of a much higher band number—hundreds or thousands of them—arranged in a narrower bandwidth (5–20 nm, each).

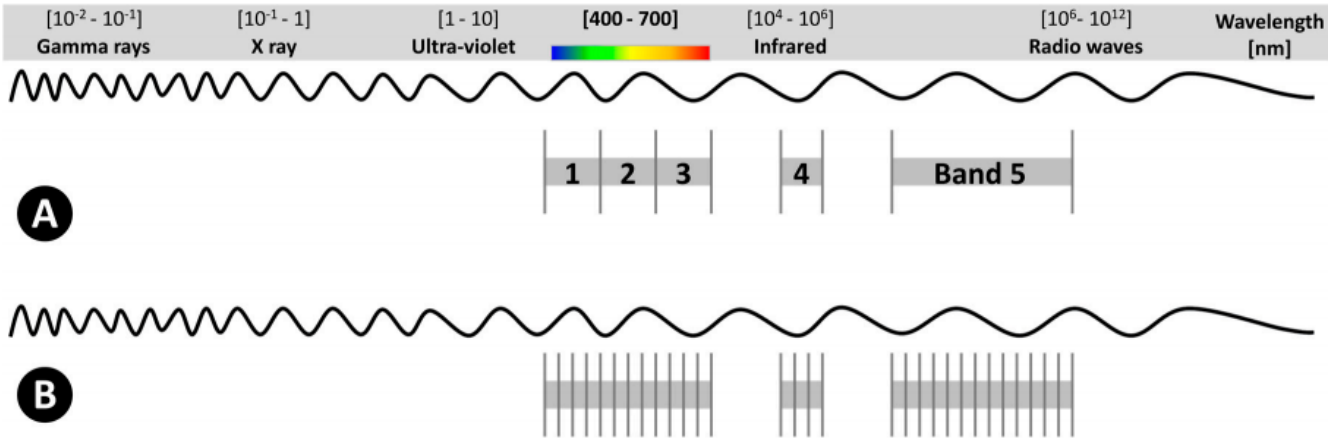

Figure 1. Spectrum representation including: (**A**) Multispectral example, with 5 wide bands; and (**B**) Hyperspectral example consisting of several narrow bands that, usually, extends to hundreds or thousands of them (image not drawn to scale, based in [14]).

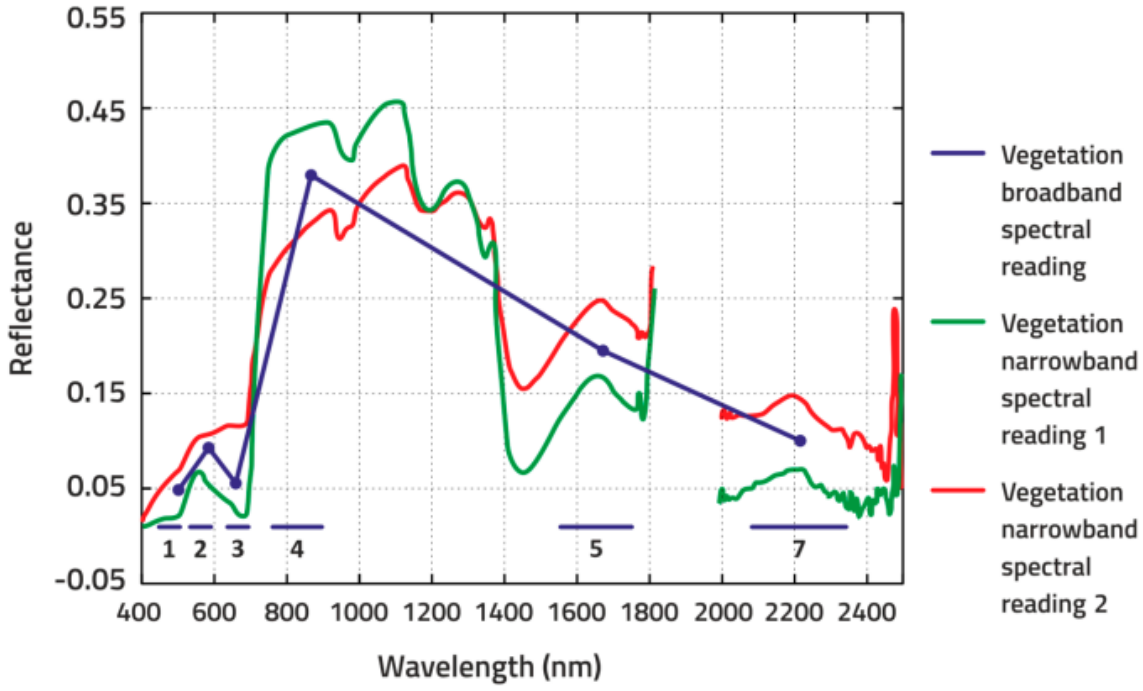

Figure 2. Broadband sensors' inability for accessing the spectral shift of the RE (670–780 nm) slope associated with leaf chlorophyll content, phenological state and vegetation stress, comparatively to wide-range narrowband ones (re-edited from [18]).

four main techniques for acquiring measurable data from a given target: by hyperspectral imaging, multispectral imaging, spectroscopy and RGB imagery.

	Spectral Information	Spatial Information
Hyperspectral Imaging	●●●	●●●
Multispectral Imaging	●●	●●●
Spectroscopy	●●●	●
RGB Imagery	●	●●●

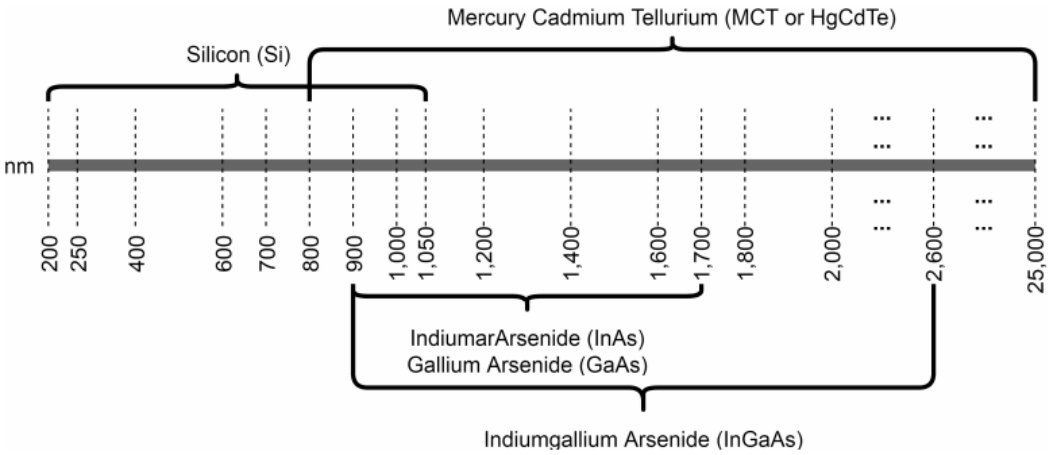

Figure 3. Materials involved in hyperspectral sensors fabrication (inspired by [43]): Silicon (Si) is used for acquiring ultraviolet, visible and shortwave NIR regions; indium arsenide (InAs) and gallium arsenide (GaAs) have a spectral response between 900–1700 nm; indium gallium arsenide (InGaAs) extends the previous range to 2600 nm; and mercury cadmium tellurium (MCT or HgCdTe) is characterized by a large spectral range and high quantum efficiency that enables reaching mid-infrared region (about 2500 to 25,000 nm) and NIR region (about 800–2500 nm).

CMOS technology is faster when acquiring and measuring light intensity.

CCD-based sensors have higher sensitivity regarding band data acquisition while, on the other hand, high grade CMOS have greater quantum efficiency in NIR.

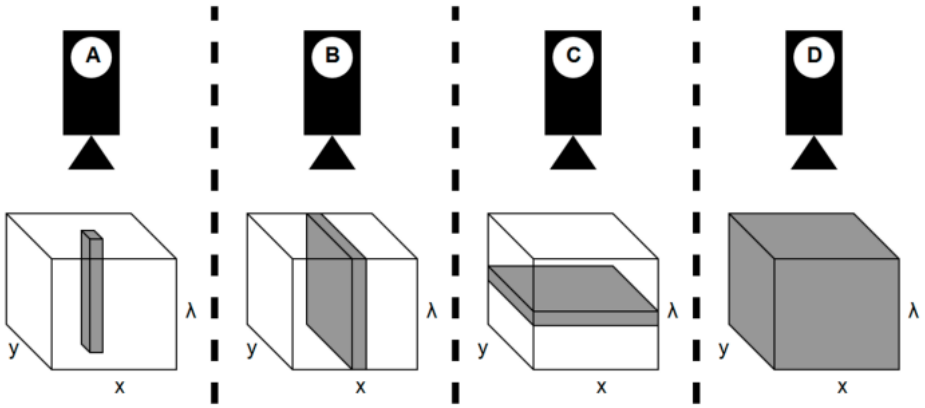

Figure 4. Hyperspectral data acquisition modes: (**A**) represents point scanning or whiskbroom mode; in (**B**) presents line scanning or pushbroom mode; (**C**,**D**) correspond to plane (or area) scanning and single shot modes, respectively (adapted from [43]).

While whiskbroom mode acquires all the bands pixel by pixel by moving the detector in the x-y space to store data in a band-interleaved-by-pixel (BIP) cube.

pushbroom mode proceeds similarly but, instead of pixel-based scanning, an entire sequence of pixels forming a line is acquired, which ends up by constituting a band-interleaved-by-line (BIL) cube. Some other pushbroom characteristics include compact size, low weight, simpler operation and higher signal to noise ratio [10]. More comparisons between pushbroom and whiskbroom modes are presented in [48]. Plane scanning mode builds a band sequential (BSQ) cube constituted by several images taken at a time, each one holding spectral data regarding a whole given x-y space.

Finally, there is a more recent mode that acquires all of the spatial and spectral data at once known as single shot. In snapshot imager seems to be related with the referenced single shot mode inasmuch as it is presented as a device that collects an entire data cube within a single integration period.

Additionally, some noteworthy issues are pointed out for each acquisition mode. Whiskbroom is a slow acquisition mode and pushbroom must use short enough time exposure to avoid the risk of inconsistencies at the spectral band level (saturation or underexposure). Plane scanning is not suitable for moving environments, while single shot was reported as an under development technology that still lacks support to higher spatial resolution.

Plant Disease Detection using Hyperspectral Imaging, Peyman Moghadam, 2017

This paper proposes the use of hyperspectral imaging (VNIR and SWIR) and machine learning techniques for the detection of the Tomato Spotted Wilt Virus (TSWV) in capsicum plants.

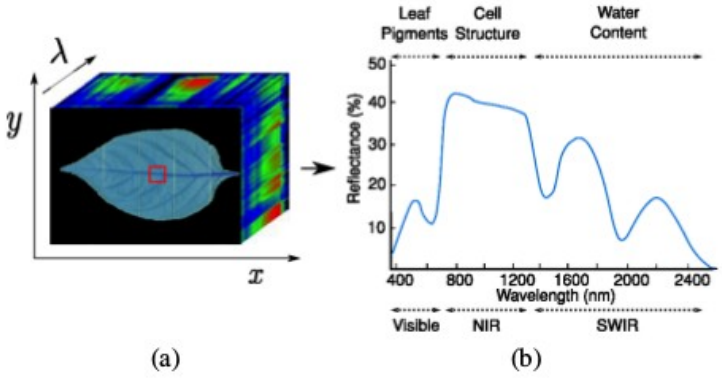

Fig. 1: (a) An example of a hypercube. (b) Spectral reflectance of a healthy plant.

Healthy plants typically absorb light in the visible range (VIS 400-700 nm) due to leaf photosynthesis pigments. The amount of light scattered in the near-infrared range (NIR 700-1000 nm) is strongly sensitive to leaf cell structure. Dominant factors influencing leaf reflectance in short-wave infrared (SWIR 1000-2500 nm) are leaf water and chemical contents.

The hyperspectral imaging system consists of two push-broom hyperspectral cameras from Headwall - the VNIR A-series and the SWIR M-series. The VNIR hyperspectral camera has a spectral range of 400-1000 nm with 324 spectral bands and a spatial resolution of 1004 pixels. The SWIR hyperspectral camera provides a spectral range of 900-2500 nm with 168 spectral bands and a spatial resolution of 384 pixels.

List of selected some Hyperspectral camera

Sr.No	Manuf.	Sensor	Spectral range (nm)	No. of Bands	Spectral Resoln	Spatial Resoln (Pixel)	Acq. mode	Wt (gms)
1	Headwall Photonics	nano	400-1000	270	6	640	p	1200
2	Senop	VIS-VNIR	400-900	380	10	1010x1010	s	720
3	Cubert GmbH	S185	450-950	125	4	50x50	s	490
4	Resonon	Pika XC2	400-1000	447	1.3	1600	p	2200
5	Hyspex	Mjolnir v-1240	400-1000	200	3	1240	p	4200
6	Bayspec	OCI-UAV-2000	400-1700	40-52	5	648x488	s	500
7	Specim	FX10	400-1000	224	5.5	1024	p	1260
8	Ximea	MQ022HG-IM-LS150-VISNIR	470-900	150	3	2048	p	32
9	Surface optics	SOC710-GX	400-1000	120	4.2	640	p	1230
10	Photon Focus	CMV2K-SM5x5-NIR	600-975	150	12	2048x1088	s	350

Manuf.	Sensor	Spectral Range (nm)	No. Bands	Spectral Resol. (nm)	Spatial Resol. (px)	Acquis. Mode	Weight (g)
BaySpec	OCI-UAV-1000	600–1000	100	<5 [b]	2048 [d]	P	272
Brandywine Photonics	CHAI S-640	825–2125	260	5 [c]	640 × 512	P	5000
	CHAI V-640	350–1080	256	2.5 [c] 5 [c] 10 [c]	640 × 512	P	480
Cubert GmbH	S 185—FIREFLEYE SE	450–950	125	4 [c]	50 × 50	S	490
	S 485—FIREFLEYE XL	355–750 450–950 550–1000	125	4.5 [c]	70 × 70	S	1200
	Q 285—FIREFLEYE QE	450–950	125	4 [c]	50 × 50	S	3000
Headwall Photonics Inc., Fitchburg, MA, USA	Nano HyperSpec	400–1000	270	6 [b]	640 [d]	P	1200 [e]
	Micro Hyperspec VNIR	380–1000	775 837 923	2.5 [b]	1004 [d] 1600 [d]	P	≤3900
HySpex	VNIR-1024	400–1000	108	5.4 [c]	1024 [d]	P	4000
	Mjolnir V-1240	400–1000	200	3 [c]	1240 [d]	P	4200
	HySpex SWIR-384	1000–2500	288	5.45 [c]	384 [d]	P	5700
MosaicMill	Rikola	500–900	50 [a]	10 [b]	1010 × 1010	S	720
NovaSol	vis-NIR microHSI	400–800 400–1000 380–880	120 180 150	3.3 [c]	680 [d]	P	<450
	Alpha-vis micro HSI	400–800 350–1000	40 60	10 [c]	1280 [d]	P	<2100
	SWIR 640 microHSI	850–1700 600–1700	170 200	5 [c]	640 [d]	P	3500
	Alpha-SWIR microHSI	900–1700	160	5 [c]	640 [d]	P	1200
	Extra-SWIR microHSI	964–2500	256	6 [c]	320 [d]	P	2600
PhotonFocus	MV1-D2048x1088-HS05-96-G2	470–900	150	10-12 [b]	2048 × 1088	P	265
Quest Innovations	Hyperea 660 C1	400–1000	660	-	1024 [d]	P	1440
Resonon	Pika L	400–1000	281	2.1 [c]	900 [d]	P	600
	Pika XC2	400–1000	447	1.3 [c]	1600 [d]	P	2200
	Pika NIR	900–1700	164	4.9 [c]	320 [d]	P	2700
	Pika NUV	350–800	196	2.3 [c]	1600 [d]	P	2100
SENOP	VIS-VNIR Snapshot	400–900	380	10 [b]	1010 × 1010	S	720
SPECIM	SPECIM FX10	400–1000	224	5.5 [b]	1024 [d]	P	1260
	SPECIM FX17	900–1700	224	8 [b]	640 [d]	P	1700
Surface Optics Corp., San Diego, CA, USA	SOC710-GX	400–1000	120	4.2 [c]	640 [d]	P	1250
XIMEA	MQ022HG-IM-LS100-NIR	600–975	100+	4 [c]	2048 × 8	P	32
	MQ022HG-IM-LS150-VISNIR	470–900	150+	3 [c]	2048 × 5	P	300

Note: [a] 380 in laboratory; [b] at FWHM; [c] by sampling; [d] Pushbroom length line (the other dimension depends on sensor's sweep distance); [e] without lens and global positioning system (GPS); P—Pushbroom; S—Snapshot.

1. https://www.headwallphotonics.com/hyperspectral-sensors

Spectral Region	Focal Length	Min. Working Dist.
UV-VIS (250-500nm)	28mm	250mm
VNIR (400-1000nm)	4.8mm	1mm
	8mm	1mm
	12mm	58mm
	17mm	42mm
	24mm	76mm (aprochromatic)
	25mm	1m (telecentric)
	37mm	400mm (telecentric)
	70mm	590mm
Extended VNIR (550-1700nm)	25mm	pending
NIR (900-1700nm) SWIR (900-2500nm)	25mm	250mm (telecentric)
	85mm	12m (telecentric)

Nano-Hyperspec®	
Wavelength range	400-1000 nm
Spatial bands	640
Spectral bands	270
Dispersion/Pixel (nm/pixel)	2.2
FWHM Slit Image	6 nm
Integrated 2nd order filter	Yes
f/#	2.5
Layout	Aberration-corrected concentric
Entrance Slit width	20 µm
Camera technology	CMOS
Bit depth	12-bit
Max Frame Rate (Hz)	350
Detector pixel pitch	7.4 µm
Max Power (W)	13
Storage capacity	480GB (~130 minutes at 100 fps)
Weight without lens, GPS (lb / kg)	1.2 / 0.5
Operating Temperature	0˚C to 50˚C

Spectral Range	VNIR (400-1000nm)		NIR (900-1700nm)		Extended VNIR (600-1700nm)	SWIR (900-2500nm)	
Micro-Hyperspec® Configuration	A-Series	E-Series	640	320	640	384	640
Focal Plane Array	Silicon CCD	sCMOS	InGaAs			MCT	
Pixel Pitch (microns)	7.4	6.5	15	30	15	24	15
Aperture	F/2.5						
Slit Length (mm)	10.5						
Dispersion/Pixel (nm)	1.9	1.63	6	12	4.1	9.6	6
Entrance Slit Width (µm)	20		25		20	25	20
FWHM Slit Image (nm)	5.8	5.8	10	10	5.5	10	8
Spectral Bands	324	369	134	67	267	166	267
Spatial Bands	1004	1600	640	320	640	384	640
Aberration-Corrected	Yes						
Max. Frame Rate (Hz)	90	250	120	346	120	450	>200
ADC Bit Depth	12	16	14			16	
Cooling	No	TE-cooled	TE-cooled			Stirling-cooled	
Digital Output Format	Base CameraLink	Full CameraLink	Base CameraLink			RS232/Base CameraLink	Base Cameralink
Weight without lens (lb / kg)	1.6 / 0.7	2.4/1.1	1.9 / 0.9			4.4 / 2.0	3.4 / 1.6
Max Power (W)	6.6	13.2	2.5	4	4	14.4	14

2. http://senop.fi/optronics-hyperspectral

sensitive for VNIR (400-1000 nm) spectral range. The HSC-2 camera is the only snapshot hyperspectral device on the market providing real spectral response in each pixel. No interpolation is used in image formation.

-Frame based snap shot Hyperspectral Camera.

-Resolution 1 Mpix. All pixels are true image pixels. No interpolation is used.

-Up to 1000 freely selectable spectral bands.

-Up to 149 frames per seconds.

TECHNICAL DATA

Parameter	Specification	Remarks
Spectral Range	400-1000 nm	The camera is sensitive for this range, application specific subranges need to be selected. Typical 500-900 nm.
Spectral FWHM	5-10 nm	
Spectral Step	0.1 nm	
Spectral Bands	up to 1000	The bands are freely selectable/programmable.
Horizontal FOV	36.8°	Diagonal 52.0°
Vertical FOV	36.8°	Diagonal 52.0°
Image Sensor	CMOS	Pixel size is 5.5 µm x 5.5 µm.
Dynamic Range	10-12 bits	
Max Image Rate (frames / s)	74 (12 bit) 149 (10 bit)	The camera exposures each band separately.
Image Resolutions	1024x1024	All pixels are true image pixels. No interpolation used.
Exposure time	Adjustable	Maximum frame rate may be limited if exposure time is long.
Memory	1TB	Shooting time with max frame rate 12 bit: 1h 45min & 10 bit: 1h 17min.
Connections	GigE RJ-45 USB 2.0 type-C Mini-Displayport v1.2 IO port with UART and 4GPIO pins MMCX for external GPS antenna (if needed)	
Weight	986 g	
Dimensions (l x w x h)	199.5 mm x 130.9 mm x 97.2 mm	
Positioning	GPS and BeiDou	With external antenna also Glonass and Galileo.
Voltage supply	7-17 VDC	Set includes AC/DC adapter with cable.
Inertial Measurement Unit	Gyroscope and 3 axis accelerometer	For accurate image stitching.
Adjustable optics	Focus distance: ∞ - 30 cm	Limited FOV 30 cm – 2 cm.
Live Use	External display can be attached	
PC-software	Senop HSI-2	Windows 7 & 10
Data export	Standard ENVI	

3. https://cubert-gmbh.com/product/uhd-185-firefly/

Camera properties	
Detector	Si CCD
Digitization	12 bit
Measurement time	down to 100 µs
Camera interface	2x Gigabit Ethernet
Hyperspectral cube rate	up to 5 cubes/s
Cube resolution	1 megapixel
Spectral throughput	2 500 spectra / cube
Processing software	included
Software development kit	included
Optical properties	
Objective	selectable
Mount	C-mount objective
Ground resolution	selectable mm - m
Physical properties	
Environment conditions	dry / non condensing
Operating temperature	0 - 40 °C
Weight	470 g
Power	DC 12 V, 15 W
Spectral properties	
Wavelength range	450 – 950nm
Sampling interval	4nm
Spectral resolution	8 nm @ 532nm
Channels	125

What you should know

The S185 uses a unique technology which establishes a fair balance between areal resolution and spectral resolution. The result is an imaging spectrometer with no need for scanning (like push broom technology) or image combination after fast filter shifts. Our technology provides clean hyperspectral images out of the box without any moving artifacts.
During the development of the FireflEYE we miniaturized our laboratory platform. The weight was reduced from 3 kg to a total weight of 470 g (including camera and optics). This was achieved by the use of lightweight and yet stable materials like aluminum and Kevlar. Due to the abstinence of any moving part, the package provides a light but longtime stable product.
In combination with an industry grade processing unit for the on air data storage and the ground communication, we achieve a ready to fly weight of as low as 840 g.

Your benefits

- Full frame hyperspectral imaging in the Vis-NIR
- No moving artifacts due to low integration time
- WiFi remote control of all parameters
- Real time hyperspectral preview on the ground
- Hyperspectral video

4. https://resonon.com/pika-l-camera

Spectral Range (nm)	400 - 1000
Spectral Resolution (nm)	2.1
Spectral Channels	281
Spatial Channels	900
Max Frame Rate (fps)	249
Bit Depth	12
Connection Options	USB 3.0
Size (cm/in)	10.0 x 12.5 x 5.3 / 3.9 x 4.9 x 2.2
Weight (kg/lb)	0.6 / 1.3
Power requirements	3.4 W
Operating Temperature Range (C/F)	5 - 40 / 41 - 104

5. https://www.bayspec.com/spectroscopy/oci-uav-hyperspectral-camera/

Key Specs		
Product Name	**OCI-UAV-1000**	**OCI-UAV-2000**
Operation Mode	Push-broom	Snapshot
Weight	~ 0.4 lb. (180 g)	
	(including a standard lens)	
Data Interface	USB 3.0 (up to 120 fps)	
Ready to fly solution provided		

https://www.bayspec.com/category/spectroscopy/hyperspectral-imaging/

7. https://surfaceoptics.com/products/hyperspectral-imaging/soc710-portable-hyperspectral-camera/

	710-VP	710-E	710-SWIR
Spectral Range (nm)	400-1000	400-1000	900-1700
Spectral Resolution (nm)	4.69	2.31	2.77
Spectral Channels	128	260	288
Spatial Channels	1040/520 (selectable)	1392/696 (selectable)	640
Dynamic Range	12/16-Bit	12-Bit	14-Bit
Cube Rate (max / nominal)	23.2 seconds	23.2 seconds	20 seconds
Weight	2.95 Kg (6.5 lbs)	3.85 Kg (8.5 lbs)	4.53 Kg (10 lbs)
Dimensions	9.5 x 16.8 x 22 cm	12.7 x 20.3 x 28 cm	12.7 x 20.3 x 28 cm

8. https://www.ximea.com/en/products/hyperspectral-cameras-based-on-usb3-xispec/mq022hg-im-ls150-visnir

Specifications:	
Resolution:	2048 × 5
Frame rates:	up to 850 lines/sec
Sensor type:	CMOS, Hyperspectral filters added at wafer-level
Sensor model:	IMEC LS150+
Sensor size:	2/3"
Sensor active area:	150+ Bands
Readout Method:	Linescan wedge
Pixel size:	5.5 µm
ADC -Bits per pixel:	8, 10 bit RAW pixel data
Data interface:	USB 3.1 Gen1 or PCI Express
Data I/O:	GPIO IN, OUT
Power consumption:	1.6 Watt
Lens mount:	C or CS Mount
Weight:	32 grams
Dimensions WxHxD:	26 x 26 x 31 mm
Operating environment:	50 °C
Spectral range:	470-900 [nm]
Customs tariff code:	8525.80 30 (EU) / 8525.80 40 (USA)
ECCN:	EAR99

9.http://www.photonfocus.com/en/products/camerafinder/camera/?no_cache=1&prid=80

Image Sensor Specifications

Manufacturer / Type	IMEC / CMV2K-SM5x5	
Technology	CMOS	
Optical format	2/3"	
Optical diagonal	12.76mm	
Resolution	2048 x 1088	
Pixel size	5.5µm x 5.5µm	
Active optical area	11.26mm x 5.98mm	
Dark current	125e^-/s	
Read out noise	13e^-	
Full well capacity / SNR	11ke^- / 105: 1	
Spectral range	Hyperspectral:	600 to 975nm (25 pass bands)
Responsivity	Hyperspectral:	454 x 10^3 DN / (J/m²) @ 715nm / 8bit
Quantum Efficiency	Hyperspectral:	> 18%
Optical fill factor	42% without micro lenses	
Dynamic range	60dB	
Characteristic curve	Linear, Piecewise linear	
Shutter mode	Global shutter	

Camera Specifications

Interface	GigE
Frame rate	42fps
Pixel clock	48MHz
Camera taps	2
Greyscale resolution	8Bit / 10Bit
Fixed pattern noise (FPN)	< 1DN RMS @ 8Bit
Exposure time range	13µs - 349ms
Analog gain	yes
Digital gain	0.1 to 15.99 (FineGain)
Trigger Modes	Free running (non triggered), external Trigger, SWTrigger
Features	Configurable region of interest (ROI), Up to 8 regions of interest (MROI), Binning for data pre processing, Decimation in y-direction, 2 look-up tables (12-to-8Bit) on user-defined image region (Region-LUT), Constant frame rate independent of exposure time, Crosshairs overlay on the image, Temperature monitoring of camera, Camera informations readable over SDK, Ultra low trigger delay and low trigger jitter, Extended trigger input and strobe output functionality, Status line in picture
Operation temperature / moisture	0°C ... + 50°C / 20% ... 80%
Storage temperature / moisture	-25°C ... 60°C / 20% ... 95%
Power supply	+12VDC (-10%) ... +24VDC (+10%)
Power consumption	< 5.1W
Lens mount	C-Mount (CS-Mount optional)
I/O Inputs	2x Opto-isolated 2x RS-422 Opto-isolated
I/O Outputs	2x Opto-isolated
Dimensions	55 x 55 x 52mm³
Mass	265g
Connector I/O (Power)	Hirose 12-pole (mating plug HR10A-10P-12S)
Connector Interface	RJ-45
Conformity	CE / RoHS / WEEE
IP Code	IP40

10. https://sentera.com/sensors/ --$4,599

Sensors	
Resolution	1x 1.2MP CMOS RGB 3x 1.2MP CMOS Mono • 655nm CWL x 40nm width • 725nm CWL x 25nm width • 800nm CWL x 25nm width
Shutter	Global
Pixel Size	3.75um
Pixel Count	1248 x 950
Lens	
FOV	50° horizontal / 39° vertical - Low Distortion
GSD @ 200'	1.8" (4.5cm)
GSD @ 400'	3.6" (9.1cm)
Size	3" x 2.45" x 1.9" (76mm x 62mm x 48mm)
Weight	170 grams
Power	5 to 26.2VDC, 12W typical
Frame Rate	1.2MP Stills: 7fps 720p Video: 20-24fps
Storage	32GB SD card per sensor • JPEG, 200,000 images per card • TIFF, 8,000 images per card
Interfaces	Ethernet, Serial/UART

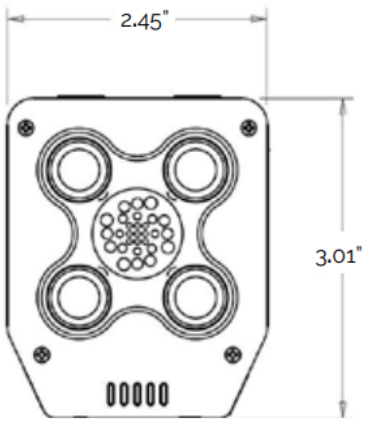

11. https://www.parrot.com/business-solutions-us/parrot-professional/parrot-sequoia#parrot-sequoia-

16 MPIX RGB CAMERA

- Definition: 4608x3456 pixels
- HFOV: 63.9°
- VFOV: 50.1°
- DFOV: 73.5°

4 1.2 MPIX GLOBAL SHUTTER SINGLE-BAND CAMERAS

- Definition: 1280x960 pixels
- HFOV : 61.9°
- VFOV : 48.5°
- DFOV : 73.7°

4 SEPARATE BANDS

- Green (550 BP 40)
- Red (660 BP 40)
- Red Edge (735 BP 10)
- Near infrared (790 BP 40)

DIMENSIONS & CHARACTERISTICS

- 59mm x 41mm x 28mm
- 72 g (2.5 oz)
- Up to 1 fps
- 64 GB built-in storage
- IMU & magnetometer
- 5 W (~12 W peak)

SUNSHINE SENSOR

- 4 spectral sensors (same filters as body)
- GPS
- IMU & magnetometer
- SD Card slot
- 47mm x 39.6mm x 18.5mm
- 35 g (1.2 oz)
- 1 W

12. https://www.micasense.com/rededge-mx/ -- **$ 5,500 USD**

Weight:	231.9 g (8.18 oz.) (includes DLS 2 and cables)
Dimensions:	8.7cm x 5.9cm x 4.54cm (3.4in x 2.3in x 1.8in)
External Power:	4.2 V DC - 15.8 V DC 4 W nominal, 8 W peak
Spectral Bands:	Blue, green, red, red edge, near-IR (global shutter, narrowband)
Wavelength (nm):	Blue (475 nm center, 20 nm bandwidth), green (560 nm center, 20 nm bandwidth), red (668 nm center, 10 nm bandwidth), red edge (717 nm center, 10 nm bandwidth), near-IR (840 nm center, 40 nm bandwidth)
RGB Color Output:	Global shutter, aligned with all bands
Ground Sample Distance (GSD):	8 cm per pixel (per band) at 120 m (~400 ft) AGL
Capture Rate:	1 capture per second (all bands), 12-bit RAW
Interfaces:	Serial, 10/100/1000 ethernet, removable Wi-Fi, external trigger, GPS, SDHC
Field of View:	47.2° HFOV
Triggering Options:	Timer mode, overlap mode, external trigger mode (PWM, GPIO, serial, and Ethernet options), manual capture mode

https://www.micasense.com/compare-sensors